Title

Viscoelastic relaxation in a heterogeneous Earth following the 2004 Sumatra–Andaman earthquake

Authors

Wiseman, Kelly
Bürgmann, Roland
Freed, Andrew M
et al.

Publication Date

2015-12-01

DOI

10.1016/j.epsl.2015.09.024

Peer reviewed

Viscoelastic relaxation in a heterogeneous Earth following the 2004 Sumatra–Andaman earthquake

Author links open overlay panel[KellyWiseman](#)[a][RolandBürgmann](#)[a][Andrew M.Freed](#)[b][ParameshBanerjee](#)[c]
Show more

https://doi.org/10.1016/j.epsl.2015.09.024

Highlights

- We model viscoelastic relaxation following the 2004 Sumatra–Andaman earthquake.
- Heterogeneous models produce observed horizontal and vertical surface displacements.
- Model rheology structure is consistent with mantle temperatures from seismic imaging.

Abstract

Consideration of the three-dimensional heterogeneity of mantle rheology allows models of viscoelastic relaxation following the 2004 Sumatra–Andaman earthquake to simultaneously fit both the observed far-field and near-field postseismic deformation. We use horizontal and vertical campaign and continuous GPS observations from the Andaman, Nicobar, and Sumatran forearc islands, mainland Sumatra, Thailand, the Malay Peninsula, the Indian Ocean, and southern India, spanning the first five years of postseismic deformation. The postseismic relaxation models consider contributions from the 2004 M_w 9.2 Sumatra–Andaman, the 2005 M_w 8.7 Nias, and 2007 M_w 8.4 Bengkulu earthquakes. Far-field motions to the east of the ruptures are equally well fit by homogeneous or laterally variable earth models. However, only models with contrasting rheology across the subducting slab, a ten-times higher mantle viscosity under the Indian Ocean lithosphere than the backarc mantle, can also produce the observed enduring postseismic uplift along the forearc and lack of far-field transient displacements in southern India. While postseismic uplift of forearc stations can also be produced by rapid and enduring down-dip afterslip, the inferred rheology structure is consistent with the distribution of mantle temperature inferred from seismic tomography.

Graphical abstract

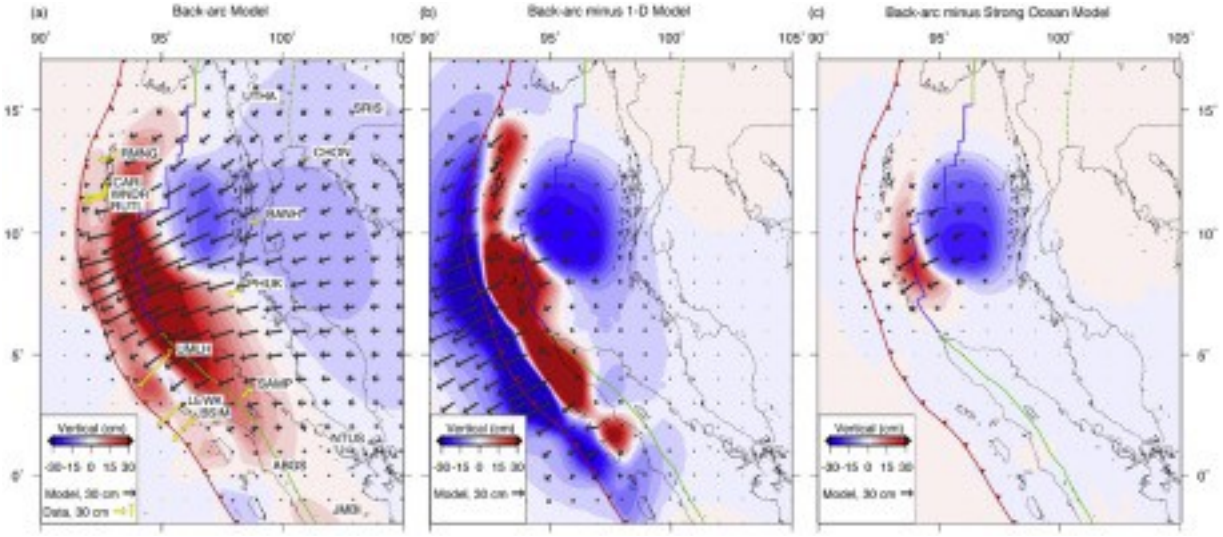

1. Download high-res image (198KB)
2. Download full-size image

- **Previous** article in issue
- **Next** article in issue

Keywords

Sumatra
subduction
earthquake cycle
mantle rheology
postseismic relaxation
finite element modeling

1. Introduction

Crustal deformation following megathrust earthquakes provides insight into the rheology of the subduction thrust fault and the relaxing mantle wedge and oceanic asthenosphere (Wang et al., 2012). Deep-seated postseismic relaxation can produce crustal deformation exceeding that from the earthquake itself in the intermediate-to-far field range. The 2004 M_w9.2 Sumatra–Andaman earthquake (Shearer and Bürgmann, 2010), and subsequent 2005 M_w 8.6 Nias (Konca et al., 2007) and 2007 M_w 8.4 Bengkulu events (Konca et al., 2008) (Fig. 1), produced large stress changes in the lithosphere surrounding the ruptures, and in the upper mantle below the rupture zones.

Postseismic deformation ensued during which various deformation processes relax the coseismic stress changes.

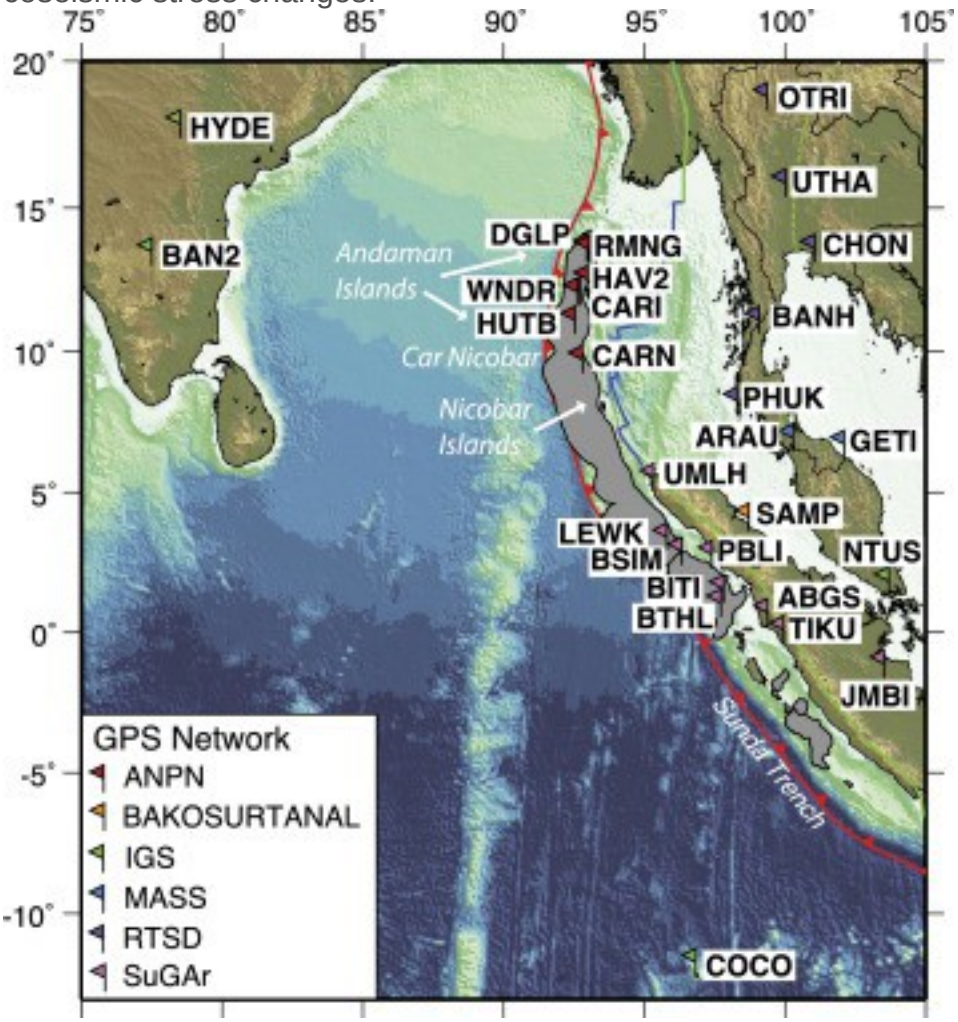

1. Download high-res image (781KB)
2. Download full-size image

Fig. 1. Overview map showing the megathrust earthquake ruptures included in the viscoelastic modeling, shaded gray, and all the GPS stations used in the study. The geodetic data come from several GPS networks, including the Andaman and Nicobar Postseismic Network (ANPN), Badan Koordinasi Survei dan Pemetaan Nasional (BAKOSURTANAL), the International GPS Service (IGS), the Malaysia Active GPS System (MASS), the Royal Thai Survey Department (RTSD), and the Sumatran GPS Array (SuGAr).

Investigations of postseismic deformation are often plagued by ambiguities between multiple processes that can be expected to contribute to the deformation field at different times and distances from the rupture, including viscous flow, localized afterslip, and poroelastic rebound (e.g., Bürgmann and Dresen, 2008). Previous studies of the

postseismic transients following the 2004 Sumatra–Andaman earthquake have primarily focused on either the near-field or the far-field postseismic deformation field, and explained the motion with dominantly afterslip (e.g., Hashimoto et al., 2006, Paul et al., 2007; Chlieh et al., 2007, Gahalaut et al., 2008), poroelastic rebound in the crust or mantle (Hughes et al., 2010, Ogawa and Heki, 2007), or viscoelastic mantle relaxation (Pollitz et al., 2006; Panet et al., 2010, Broerse et al., 2015). Several studies argued for the importance of contributions from multiple mechanisms (e.g., Paul et al., 2012, Hoechner et al., 2011, Hu and Wang, 2012). Hoechner et al. (2011), Panet et al. (2010) and Broerse et al. (2015) find that no or modest afterslip are needed to explain GPS displacements and GRACE gravity-change measurements, if a rapidly relaxing Burgers viscoelastic rheology is considered. Here we consider both near-field and far-field measurements of five years of postseismic deformation since 2004 to explore the underlying relaxation processes.

Models of viscous relaxation in a vertically stratified earth without a strong subducting slab predict horizontal surface displacements towards the downdip end of the coseismic rupture plane (e.g., Pollitz et al., 2008). Postseismic subsidence from viscous relaxation in such a layered earth model is concentrated along the zone above the rupture bottom, surrounded by a broad regional uplift which grades into a very modest zone of far-field subsidence (Fig. 2). The deformation magnitude and distribution are dependent on the earthquake source, mantle rheology, and the thickness of the elastic lithosphere. Such 1-D rheology models have been successful in matching far-field motions of GPS stations to the east of Sumatra (e.g., Pollitz et al., 2006; Panet et al., 2010, Hoechner et al., 2011, Broerse et al., 2015), but predict subsidence for near-field GPS stations on forearc islands along the Andaman–Sunda subduction zone, where observations indicate rapid postseismic uplift. Thus, when using layered earth models, either a rupture model with a shallower depth of peak coseismic slip (Hoechner et al., 2011) or rapid afterslip downdip of the rupture (e.g., Paul et al., 2012) are needed to allow for also fitting the near-field GPS data.

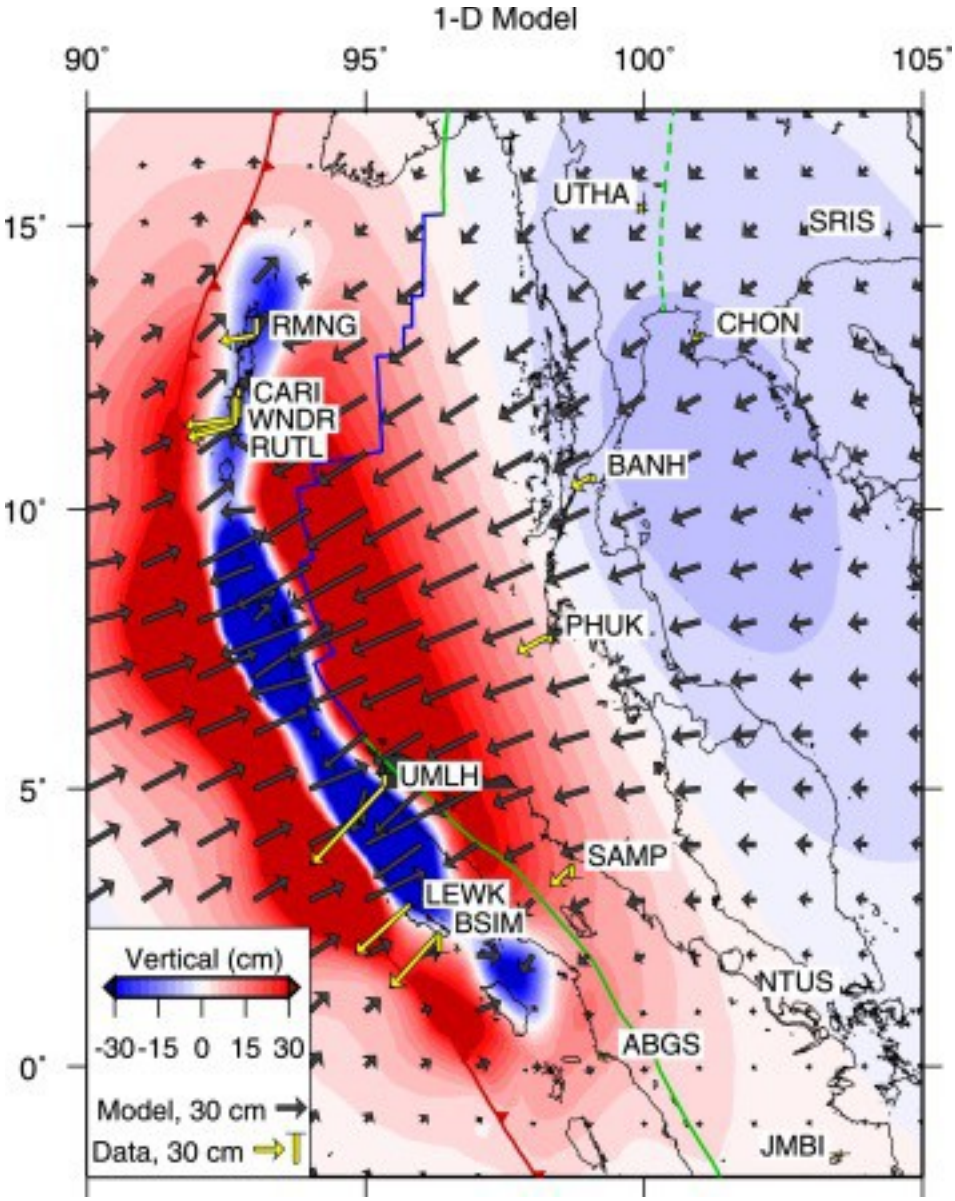

1. Download high-res image (630KB)
2. Download full-size image

Fig. 2. Observed cumulative displacements from 2005 to 2010 associated with postseismic deformation from the 2004, 2005, and 2007 megathrust earthquakes. Yellow arrows and bars show observed horizontal and vertical 5-year displacements, respectively. Coseismic displacements from the megathrust earthquakes and interseismic rate estimates have been removed from the GPS data. Black arrows show horizontal model displacements, color contours indicate predicted vertical motions from a model of cumulative viscoelastic mantle relaxation following the three earthquakes using a 1-D layered earth model. (For interpretation of the references to color in this figure legend, the reader is referred to the web version of this article.)

We can expect the rheology of the lithosphere and upper mantle in Southeast Asia to have significant 3-D heterogeneity based on geological and seismological considerations. The oceanic lithosphere thickness is dependent on the age of the oceanic crust, which varies by ~70 Ma along the Andaman–Sunda Trench (Müller et al., 1997), but in general oceanic lithosphere is thinner than the continental lithosphere of the Sunda Plate interior. The Andaman Sea is an active back-arc basin (Curray, 2005), and low seismic velocities in this region imply a locally warmer, weaker mantle (Shapiro et al., 2008). Fig. 3 shows cross-sections of seismic shear-wave velocity and a map of mantle temperature at 50 km depth estimated from surface-wave tomography of the upper mantle surrounding the subduction zone (modified from Shapiro et al., 2008; Shapiro, pers. comm., 2013). The temperature estimate is based on Shapiro and Ritzwoller (2004), who describe the conversion from isotropic seismic velocities to temperature based on thermoelastic properties of mantle materials obtained in the laboratory. Assuming that the velocity changes are primarily due to temperature variations in the mantle, this indicates lateral temperature differences of as much as 500 °C from the cold sub-Indian Ocean lithosphere and subducting slab to the warm Sumatra–Andaman back-arc region. Variations of inferred temperature within the Indian Ocean plate are consistent with plate age increasing from the fossil Wharton Ridge and the effect of hot spot activity associated with the Ninety East Ridge (Shapiro et al., 2008). The importance of lateral variations of mantle temperature and rheology that can be inferred from seismic tomography has also been recognized in global models of post-glacial rebound (Paulson et al., 2005).

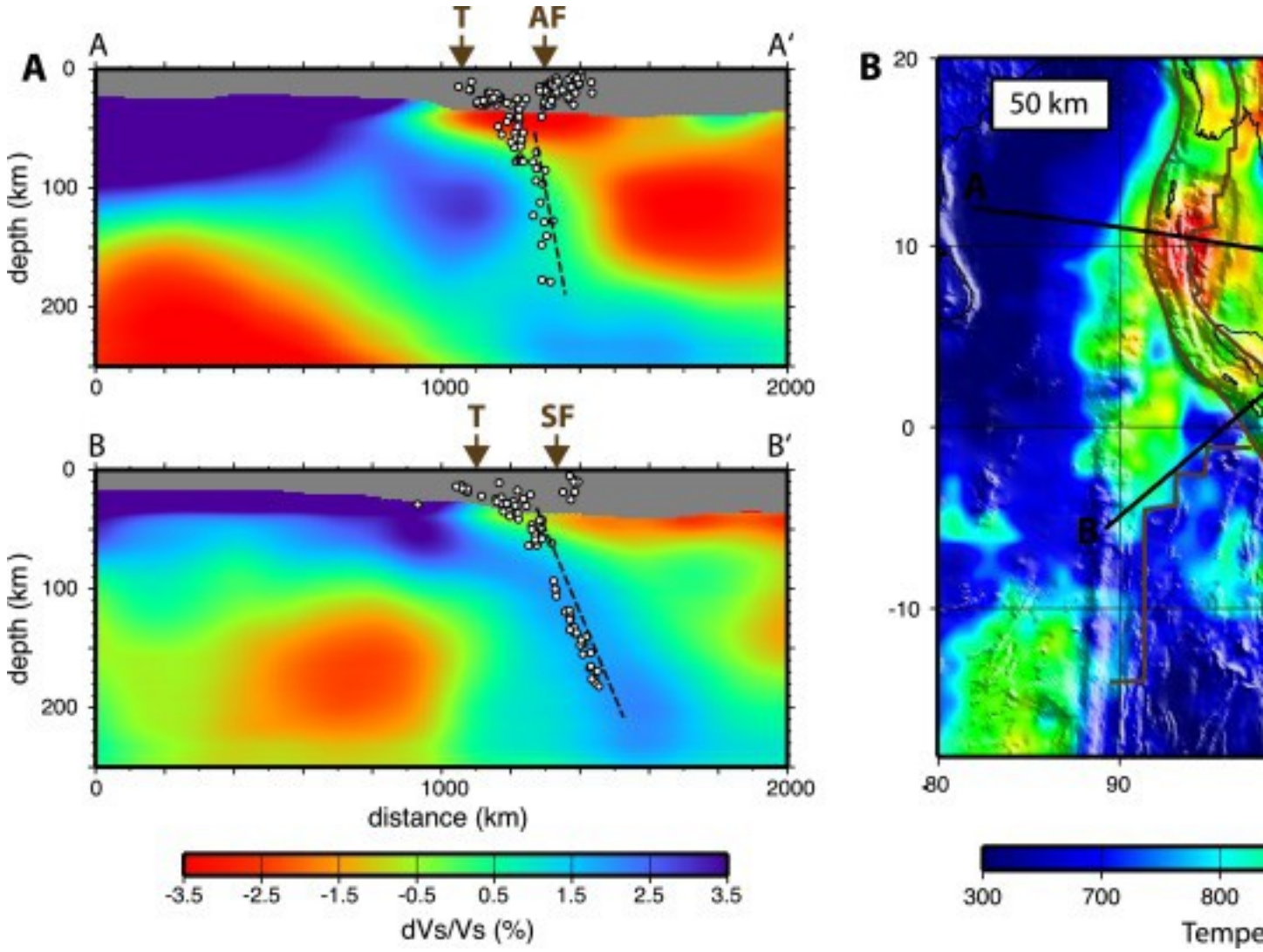

1. Download high-res image (889KB)
2. Download full-size image

Fig. 3. Surface wave tomography model of Southeast Asia from Shapiro et al. (2008). (A) Cross sections of shear-wave velocity across the Andaman–Sunda subduction zone. The locations of section lines are shown in (B). (B) Temperature at 50 km depth estimated from seismic velocity model (N. Shapiro, pers. comm., 2013) using approach of Shapiro and Ritzwoller (2004).

Pollitz et al. (2008) used an aspherical perturbation of a spherically stratified viscoelastic earth model to produce a first-order heterogeneous model that included a high-viscosity dipping slab and reduced asthenosphere viscosity in the mantle wedge. They find that while this model improved the fit to far-field vertical motions, it did not fit the near-field horizontal or vertical data. Hu and Wang (2012) present a spherical-Earth viscoelastic finite element model of the short-term postseismic deformation coming to similar

conclusions, arguing for afterslip to improve the fit to the near-field motions. Here, we test a variety of earth structures, using a finite element model approach, ranging from a simple 1-D layered model to a 3-D model that includes an elastic subducting slab, contrasting mantle asthenosphere viscosities across the subduction zone, and a low-viscosity back-arc spreading center, to determine the effects on surface deformation in the near-to-far field range. We find that models with heterogeneous rheology informed by the tomographic model of Shapiro et al. (2008) appear to reconcile the displacements of near- and far-field GPS stations and suggest that viscoelastic relaxation dominates the postseismic deformation. The contribution of afterslip is likely to be localized in zones of low megathrust coupling near the recent ruptures (Avouac, 2015).

2. Geodetic observations of coseismic and postseismic deformation

We have collated a combination of continuous and campaign GPS data from throughout Southeast Asia spanning the first five years following the 2004 Sumatra–Andaman earthquake (Fig. 1). The GPS positions are calculated in the ITRF 2005 reference frame and continuous interseismic velocities due to the plate motion between the subducting Indo-Australian Plates and the overriding Sunda Plate have been removed from the time series. The removed interseismic velocities are either motions recorded at the individual sites before the 2004 earthquake, or inferred from the Apel (2011) block model that considers rigid rotations of fault-bounded blocks and elastic strain accumulation near the faults. We also removed coseismic offsets from the 2005 Nias and 2007 Bengkulu earthquakes. Fig. 4shows the coseismic station displacements from the three earthquakes together with the predicted displacements from elastic dislocation models of the ruptures in a layered earth. Below, we describe displacement time series of near-field stations, which are located on the Andaman and Nicobar island chain as well as on forearc islands of northern Sumatra, intermediate-field sites on mainland Sumatra, and far-field observations in Thailand, Malaysia, Singapore, and southern India. Fig. 5 shows representative time series of stations BAN2, CARI, LEWK and BANH (see Fig. 1 for station locations). All time series are shown in Figs. S1 to S6. Cumulative five-year (2005–2010) displacements of representative stations with coseismic offsets and interseismic motions removed are shown in Fig. 2.

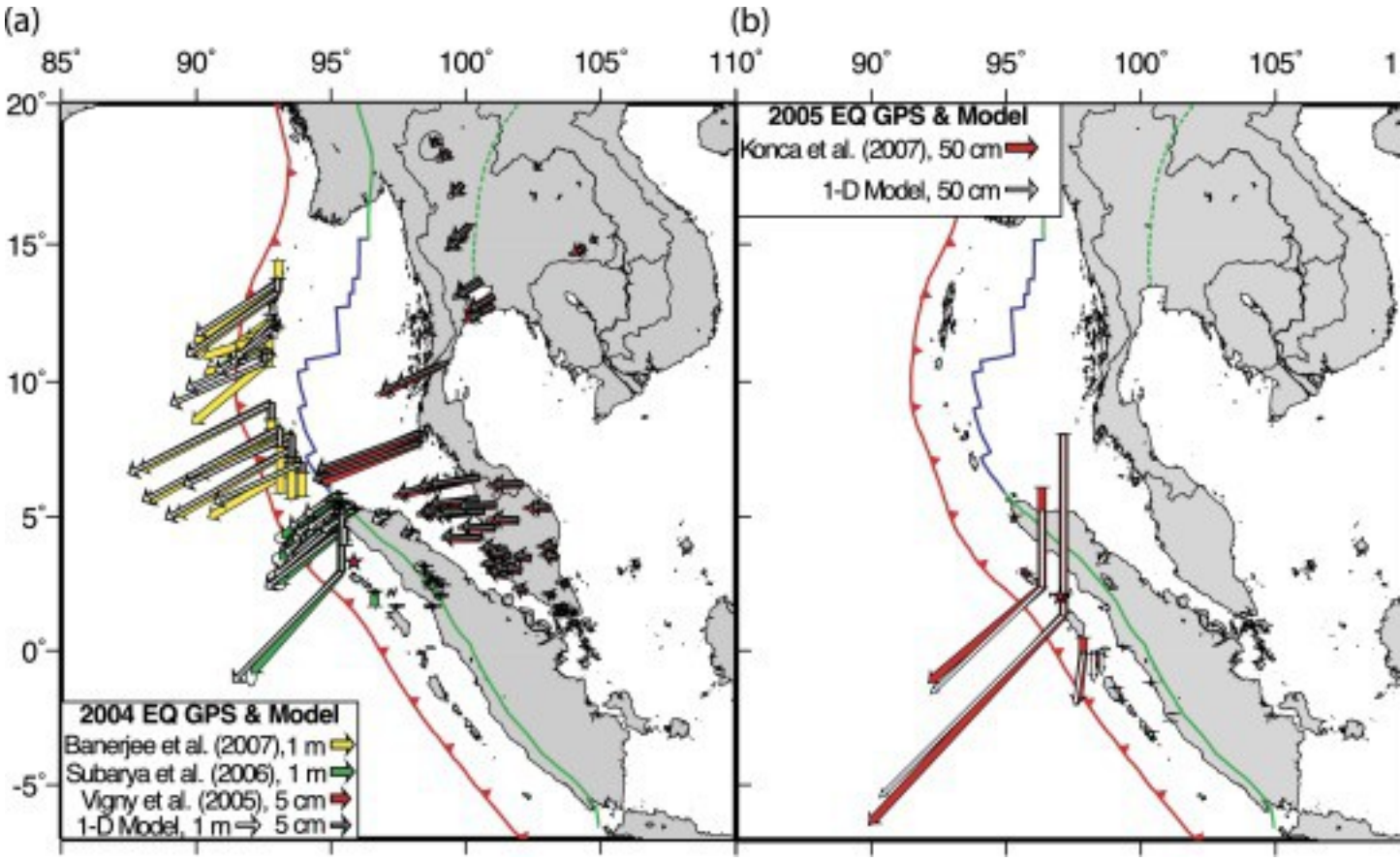

1. Download high-res image (786KB)
2. Download full-size image

Fig. 4. Elastic layered-earth model fits to the coseismic GPS data for the (a) 2004 M_w 9.2 Sumatra–Andaman earthquake (Banerjee et al., 2007, Subarya et al., 2006, Vigny et al., 2005), (b) 2005 M_w 8.8 Nias earthquake (Konca et al., 2007), and (c) 2007 M_w 8.4 and 7.9 Bengkulu earthquakes (Konca et al., 2008). There are minimal differences when using the other earth models.

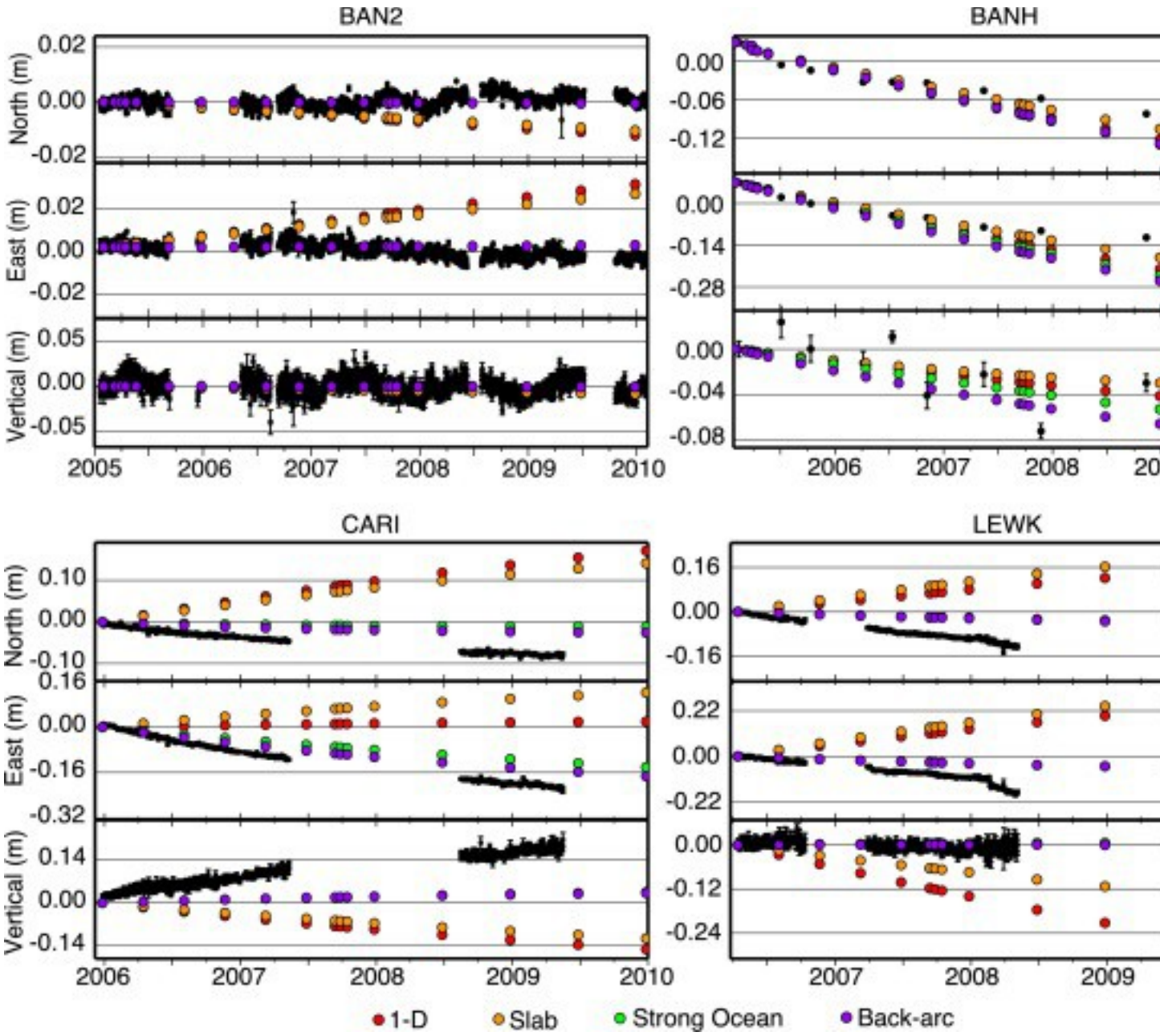

1. Download high-res image (718KB)
2. Download full-size image

Fig. 5. Examples of measured postseismic time series (black circles with one-sigma error bars), corrected for interseismic rates and coseismic offsets, from stations in southern India (BAN2), the Andaman Islands (CARI), on the Sumatra forearc island Simeulue (LEWK), and in Thailand (BANH). See Fig. 1 for station locations. Colored circles are predicted displacements from the models described below (see legend at bottom). (For interpretation of the references to color in this figure legend, the reader is referred to the web version of this article.)

2.1. Near-field GPS observations

The 2004 earthquake produced between ~1.4–4.7 m of southwestward horizontal displacement at the Andaman Islands sites, located directly above the rupture zone. The vertical displacement ranged from 0.9 m of subsidence to 0.9 m of uplift (Fig. 4a, data from Banerjee et al., 2007). The earliest postseismic observations start 15–40 days after the earthquake. The postseismic time series (Paul et al., 2012) of representative sites with interseismic background rates removed are shown in Fig. S1. The postseismic deformation rapidly decayed for the first year and then the trend became more linear. During the first five years, the cumulative horizontal displacements were ~0.4–0.6 m oriented approximately westward, and between 0.2–0.3 m of uplift (Fig. 2).
The 2004 earthquake produced up to ~5.7 m of southwestward horizontal displacement at the islands offshore of northern Sumatra, near the southern termination of the rupture, and up to 2.1 m of uplift (Fig. 4a, data from Subarya et al., 2006). Three months later, the Nias earthquake ruptured the segment of the Sunda megathrust just south of the 2004 rupture and produced up to ~4.5 m of southwestward horizontal motion and 2.9 m of uplift (Fig. 4b, data from Konca et al., 2007). Rapidly decaying postseismic deformation was also observed following the Nias earthquake, and Hsu et al. (2006) modeled the first 11 months of deformation as aseismic afterslip located both updip and downdip of the rupture, with geodetic moment equivalent to M_w 8.2. Fig. S2 shows the time series for the island sites starting one year after the 2005 earthquake, when the rapidly decaying motion has decreased. During the next four years, the sites continue to move towards the trench on the order of centimeters per year, while orientation and magnitude of vertical deformation vary greatly.

2.2. Intermediate-field GPS observations

The sites on the northernmost tip of Sumatra experienced between ~1.7–3.7 m of southwestward horizontal coseismic displacement in 2004, with ~0.1–0.6 m of subsidence (shown in Fig. 4a, data from Subarya et al., 2006). These sites only moved a few centimeters during the 2005 earthquake. SAMP, on the eastern coast of northern Sumatra, experienced 10–20 cm of trenchward motion during both the 2004 and 2005 earthquakes, with only ~1 cm of uplift. These sites continued to displace between ~0.3–1.1 m trenchward during the first five years following the 2004 earthquake (representative sites shown in Fig. 2). The sites on the western coast of central Sumatra moved <1 cm during the 2004 earthquake, but had coseismic displacements on the order of centimeters for both the 2005 and 2007 earthquakes. JMBI on the eastern coast displaced <1 cm in the 2004 and 2005 earthquakes and a few centimeters during

the 2007 earthquake. These central Sumatran sites had transient horizontal motions on the order of centimeters during the first five years following the 2004 earthquake, with no observable vertical deformation (time series starting one year after the Nias earthquake are shown in Fig. S3).

2.3. Far-field GPS observations

A wide range of coseismic 2004 horizontal displacements were observed in Thailand and the Malay Peninsula, across the Andaman Sea from the 2004 rupture (Vigny et al., 2005, Banerjee et al., 2007). Northern Thailand displaced a few centimeters, central Thailand ~6–8 cm, and the peak displacements of ~0.3 m were observed on the island of Phuket, offshore of southern Thailand (Panumastrakul et al., 2012). Northern Malaysia had ~8–15 cm of horizontal displacement and Singapore, at the southern end of the Malay Peninsula shifted by 2 cm (shown in Fig. 4a, data from Vigny et al., 2005). PHUK and the sites further south experienced southward coseismic displacement during the 2005 earthquake on the order of centimeters. NTUS, in Singapore, also displaced a few centimeters trenchward during the 2007 earthquake, followed by a rapidly decaying transient on the order of a few months (see time series in Fig. S5). These Thai and Malay Peninsula sites experienced more cumulative postseismic deformation than coseismic displacements, peaking at PHUK with ~0.4 m of southwestward motion from 2005 to 2010 (see time series for BANH in Fig. 5and all backarc sites in Figs. S4 and S5).

The very far-field sites in the Indian Ocean and India experienced very little coseismic and postseismic deformation (Fig. S6). The south Indian sites shifted eastward ~1 cm during the 2004 earthquake, and have moved another ~1 cm eastward in the next five years (e.g., BAN2 in Fig. 5). COCO, in the Indian Ocean offshore of southern Sumatra displaced <1 cm during the 2004 earthquake, and ~1 cm north during the 2007 earthquake. It moved another ~1 cm by 2010.

3. Viscoelastic modeling of postseismic deformation

3.1. Finite element model

We use the Abaqus finite element modeling software to model the postseismic deformation following the 2004, 2005, and 2007 megathrust earthquakes. The three-dimensional geometry of the model is shown in Fig. 6. The subduction interface, used both as the fault contact and for a rheological boundary, is based on the Sumatra–Java slab model from Slab1.0 (Hayes et al., 2012). Slab1.0 is a compilation of 3D subduction geometries, based on a probabilistic non-linear fit to a combination of independent data

sets including active source seismic data, several earthquake catalogs, high-resolution bathymetry, and sediment thickness data. We contoured the Sumatra–Java slab surface at the seafloor surface and depths of 20, 30, 50, 70, 150, 300, and 500 km. We do not consider seafloor bathymetry or topography. To simplify the slab geometry, we manually decimated the Slab1.0 model along strike, keeping the prominent structural features intact while segmenting the slab surface on average every 240 km. We extend the Sumatra slab beyond the 10° N limit of Slab 1.0 along the strike of the Andaman trench until 24° N, while assuming the same slab dips as at the northern extent of the Slab1.0 model. We use the Java slab surface until 115° E. We additionally extend the model volume, and subduction interface, 1000 km to the north and east to ensure that our GPS sites are located far from the model boundaries. The western edge of the model volume is ~3000 km west of the 2004 rupture and the eastern edge of the model is ~2500 km east of the 2007 rupture. The total rectangular volume is ~6600 km×~5900 km×500 km. We use quadratic tetrahedral elements for the mesh, with between ~400,000–450,000 thousand elements for the various 3-D models (example mesh shown in Fig. 6). For all of the models, the boundary conditions are enforced zero displacements at the lateral and bottom boundaries. Tests show these boundaries to be of sufficient distance from the region of interest that the boundary conditions to not influence model results.

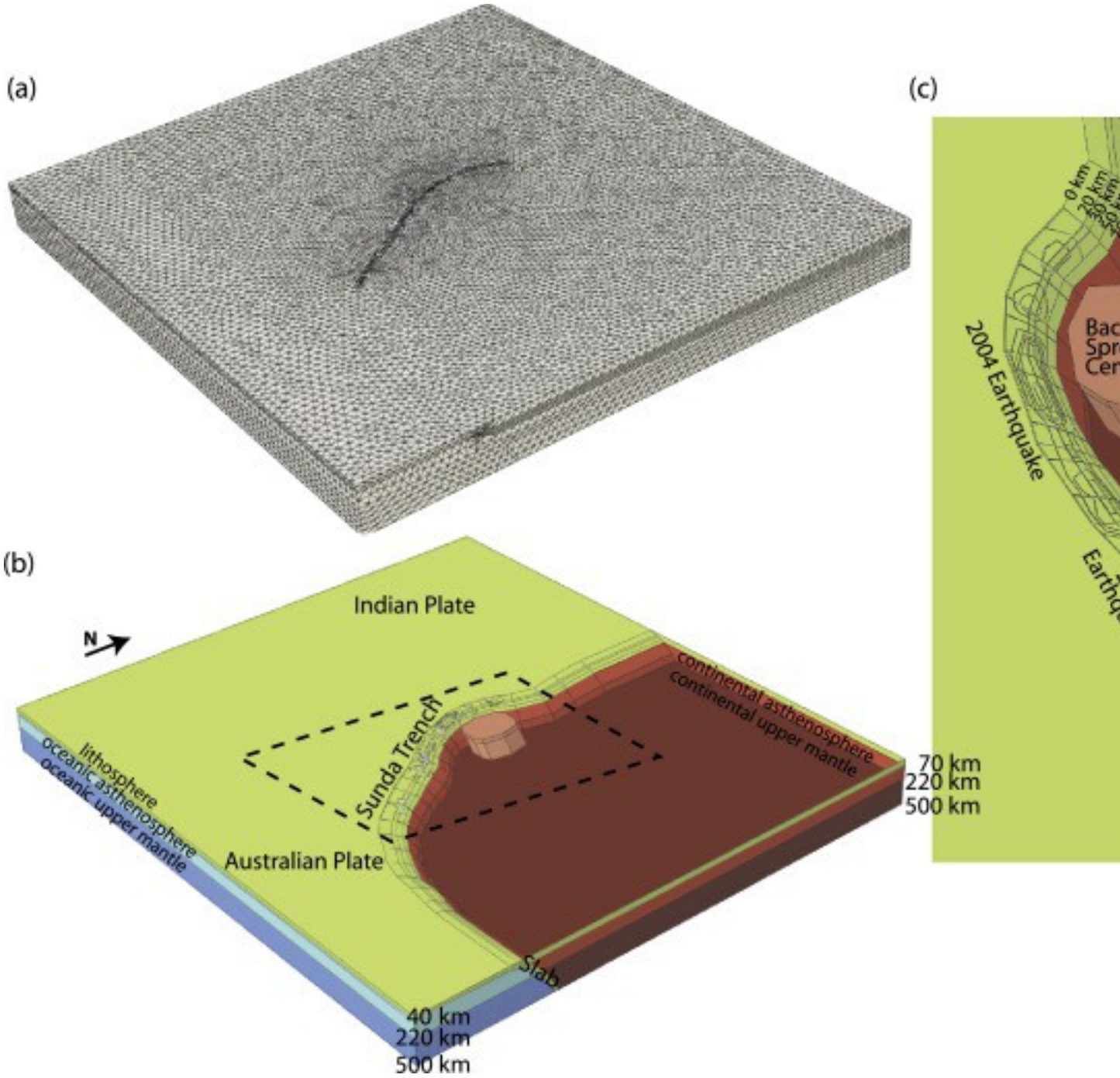

1. Download high-res image (1MB)
2. Download full-size image

Fig. 6. Finite element model geometry. (a) Finite element model mesh used in the backarc model. (b) View of three-dimensional geometry used in the weak back-arc finite element model. Dashed polygon shows approximate area of the close-up view in (c). (c) Close-up view of model geometry showing the distribution of coseismic slip of the 2004,

2005 and 2007 megathrust earthquakes considered in the models of co- and postseismic deformation.

3.2. Earthquake source models

We adapt previously published source models for the megathrust earthquakes for our coseismic input. We start by projecting the 1, 3, 6, 9, and 15 m slip contours from the geodetically constrained Chlieh et al. (2007) source model of the 2004 earthquake onto our slab interface (Fig. 6). The slip contours are manually adjusted to fit within our fault segment constraints. Then we adjust the slip magnitudes at each contour by forward modeling until we get a good fit to the geodetic data (Fig. 4a). We are actually able to fit the Andaman and Nicobar Island coseismic displacements better than the original Chlieh et al. (2007) model. We are also able to fit the far-field geodetic data, indicating that our model volume is large enough to avoid artifacts from our zero displacement boundary conditions. We use the same approach for the 2005 and 2007 earthquakes, projecting the 1, 3, and 6 m slip contours from the Konca et al. (2007) model of the 2005 earthquake and Konca et al. (2008) source models of the 2007 events, both of which are constrained by both geodetic and seismic data. We include both the M_w 8.4 mainshock and the M_w 7.9 aftershock for the 2007 earthquake source. We refrain from including the small, deep, and outlying 1-m slip contours for the 2005 and 2007 earthquakes, thus our fits to the geodetic data (Figs. 4b and 4c) are slightly worse than the original model fits.

3.3. Viscoelastic model geometry and rheology

We explore forward models of viscous relaxation in response to the coseismic stress changes in increasingly heterogeneous characterizations of the first-order earth structure of the Andaman–Sunda–Java subduction system and adjoining plates. The simplest model we test is a 1-D layered model (Fig. 7a). It includes a 70-km-thick elastic lithosphere above a ductile asthenosphere and upper mantle. The asthenosphere and upper mantle have the same viscosity in this 1-D model, and in the more complex models discussed next. We justify this simplification based on the postseismic deformation study by Panet et al. (2010), who modeled the first ~3 yr of far-field GPS data and regional GRACE gravity signal following the 2004 and 2005 megathrust earthquakes, and found that constant steady-state viscosity throughout the entire ductile portion of the mantle provides the best fit to the GRACE data. Since this study is focused on deducing the impacts of 3-D earth heterogeneity in viscoelastic models, we chose to use a simple Maxwell rheology for the ductile portions of the mantle, even

though the rapidly decaying time series are better fit by models in which the effective viscosity increases with time (e.g., Pollitz et al., 2008, Panet et al., 2010, Hu and Wang, 2012). Using a forward modeling approach, we optimized the steady-state viscosity to fit the far-field GPS sites in Thailand and the Malay Peninsula. We tested viscosities ranging between 4×1017 Pas and 8×1018 Pas, the values used in the Panet et al. (2010) study for the transient and steady-state viscosity in their bi-viscous Burgers body rheology model. The preferred steady-state viscosity to fit the first five years of far-field postseismic deformation is 3×1018 Pas (Fig. 2).

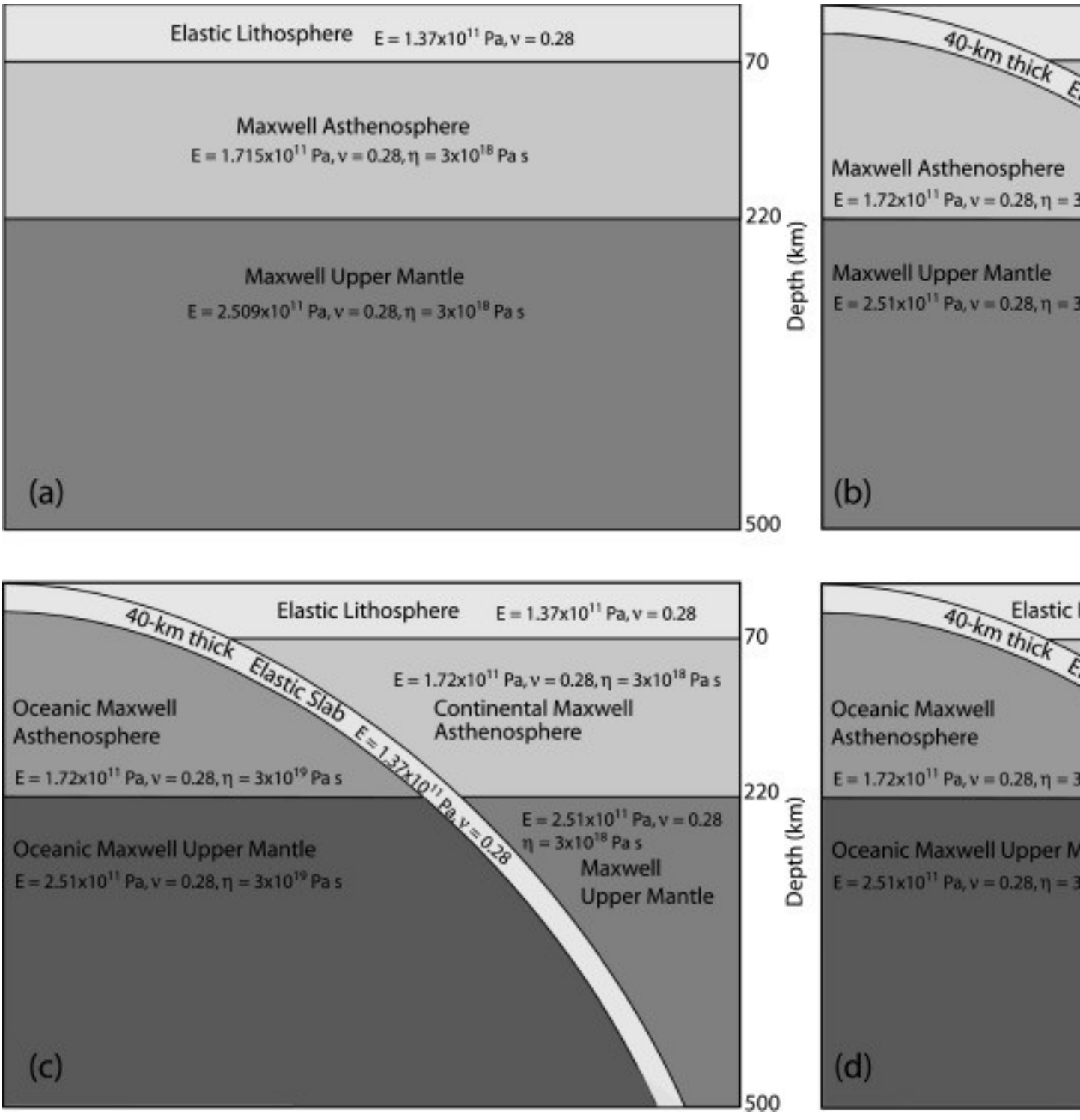

1. Download high-res image (737KB)
2. Download full-size image

Fig. 7. Cross-sectional schematics illustrating 1-D and heterogeneous earth models considered in this study and the rheological parameters used in the FEM forward models (E, Youngs modulus; *v*, Poisson's ratio; *η*, viscosity). (a) The best-fit 1-D layered

earth model. Model modifications to improve the fit to the data include (b) the addition of the elastic subducting slab (slab model), (c) increased viscosity of the mantle below the oceanic lithosphere (strong ocean model), and (d) contribution of a low-viscosity zone below the back-arc spreading center (back-arc model). See text for model description and comparison.

In the rest of the earth models, we add 3-D geometrical complexity in an attempt to improve the fit to the near-to-intermediate field postseismic observations. In the first heterogeneous earth model, we include a subducting slab (Fig. 7b). The elastic slab is 40 km thick, and follows the geometry of the slab interface as described in the Finite Element Model section above. The mantle rheology is the same on both the oceanic and continental sides of the slab, and we use the same Maxwell viscosity of 3×1018 Pas as determined for the 1-D model.

In the next iteration, we examine a different Maxwell rheology on either side of the slab (Fig. 7c). Wang (2007) finds that a strong oceanic mantle, with an order of magnitude higher viscosity than the continental mantle, is necessary to fit the uplift histories of the Washington coast following the last great Cascadia megathrust earthquake and Hu et al. (2004) come to similar conclusions considering the postseismic coastal uplift following the great 1960 Chile earthquake. The shear-wave tomography study by Shapiro et al. (2008), that spans the Andaman–Sunda–Java subduction zone, also suggests a colder and/or dryer, thus stronger, oceanic asthenosphere based on higher shear wave velocities for depths ranging from ∼25–150 km (Fig. 3). The shear-wave speed contrast between the oceanic and continental sides of the trench is more pronounced along the Andaman segment of the subduction zone than in the Sumatran segment. For simplicity we neglect such second-order variations, and assume a uniform oceanic mantle viscosity ten times larger than the backarc mantle viscosity. In the final model, we add a low-viscosity zone representing the Andaman back-arc spreading center (Fig. 6, Fig. 7d). We approximate the geometry of the low-viscosity zone based on the Shapiro et al. (2008) low shear-wave velocity region beneath the Andaman Sea (Fig. 3). Shapiro et al. (2008) could not constrain the seismic velocities shallower than ∼40 km depth, so the low-velocity zone may in actuality be shallower than we are currently modeling it. We assume a steady-state viscosity of 1.5×1018 Pas, equal to half the continental mantle viscosity, for a first-order evaluation of the effect of this feature on the postseismic deformation.

4. Model results

4.1. 1-D model

The 1-D model produces horizontal deformation at the earth's surface oriented towards the downdip end of the coseismic rupture planes (Fig. 2). Modeled subsidence is localized along the zone above the rupture bottom, surrounded by zones of regional uplift and a broad zone of modest subsidence east of the Malay Peninsula. The magnitude of horizontal and vertical displacements are close to symmetric about the downdip end of the rupture planes. Fig. 2compares the cumulative five-year deformation from viscoelastic relaxation in a vertically layered earth structure with the GPS observations that span the entire 2005–2010 time period. Figs. S1 through S6 show the fit of the 1-D model predictions (and the other models considered) to the GPS time series, generally starting one year after the most recent earthquake affecting a station to avoid the early period of rapid relaxation that is due to afterslip and/or low early transient viscosity. The near-field GPS observations fit the model very poorly, with the opposite sense of horizontal and vertical motion. The intermediate-field sites on Sumatra have the correct sense of horizontal motion, but wrong sense of vertical displacement. The far-field sites in Thailand and the Malay Peninsula have the correct sense of motion, except for the vertical at the western-most site PHUK which subsided by ∼8 cm, but is predicted to uplift by about 4 cm. The layered model with uniform viscosity across the subduction zone substantially over-predicts the cumulative postseismic deformation at the Indian sites.

4.2. Slab model

Adding the 3-D structure of the elastic, subducting slab increases the eastward component of deformation in the near field and shifts the pivot line separating uplift from subsidence further east (Fig. 8). The addition of the elastic slab has a greater influence on vertical than on horizontal motions (Fig. 8b). It reduces the symmetry of the uplift pattern, so that there is much more postseismic uplift near the trench than in the Andaman back-arc basin. The north and vertical components of deformation improve at the Andaman sites, but the fit to the east component worsens (see CARI in Fig. 5 and Fig. S1). BITI and LEWK have improved fits to the vertical deformation (see LEWK in Fig. 5 and Fig. S2), but otherwise the Sumatran Islands sites do not show improvement. The far-field sites are minimally affected by the addition of the slab (Fig. 8b).

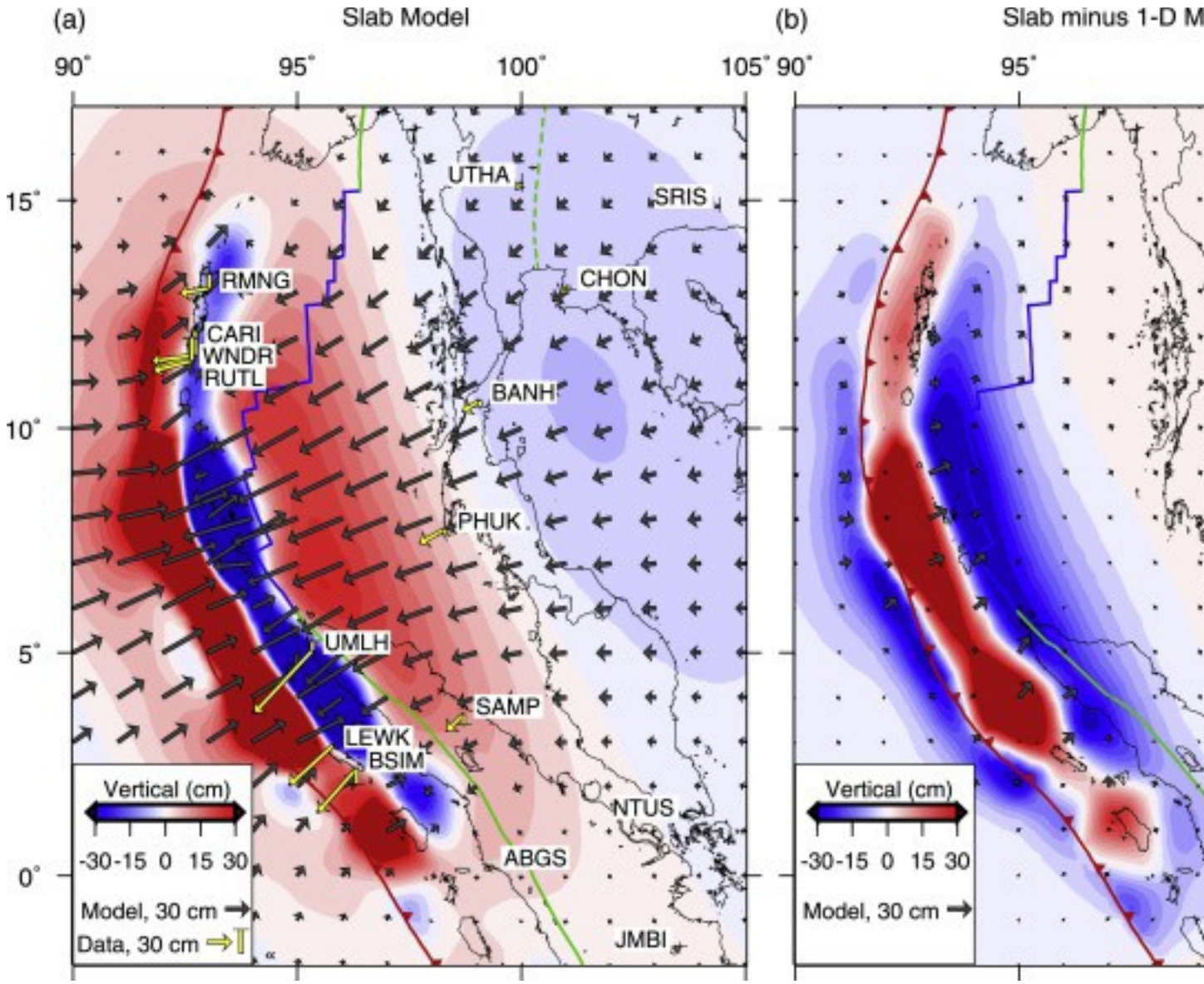

1. Download high-res image (984KB)
2. Download full-size image

Fig. 8. (a) Five years of cumulative viscoelastic relaxation from the 2004, 2005, and 2007 megathrust earthquakes using an earth model in which the elastic subducting slab is added to the layered starting model (Fig. 7b). Interseismic velocities and coseismic displacements from the 2005 and 2007 megathrust earthquakes have been removed from both the model and GPS data. (b) The difference between the slab earth model and the 1-D earth model cumulative viscoelastic relaxation.

4.3. Strong ocean model

Adding a higher-viscosity oceanic mantle dramatically changes the near-field deformation. There is added trenchward motion and uplift at the location of the forearc

islands and subsidence near the trench (Fig. 9, Figs. S1–S6). This model produces the correct orientation of horizontal motion at the forearc islands, and the correct sense of vertical motion at all of the sites except BSIM. The model also improves the fit to the vertical data at the northern Sumatra site UMLH. Deformation seaward of the trench is substantially reduced for the 5-yr observation period (Fig. 9), in agreement with the lack of postseismic deformation observed in southern India (see BAN2 in Fig. 5 and Fig. S6). If we further increase the contrast in asthenosphere viscosity across the slab we find little further change in the five-year model displacements, given the long relaxation times of the oceanic mantle implied by such models.

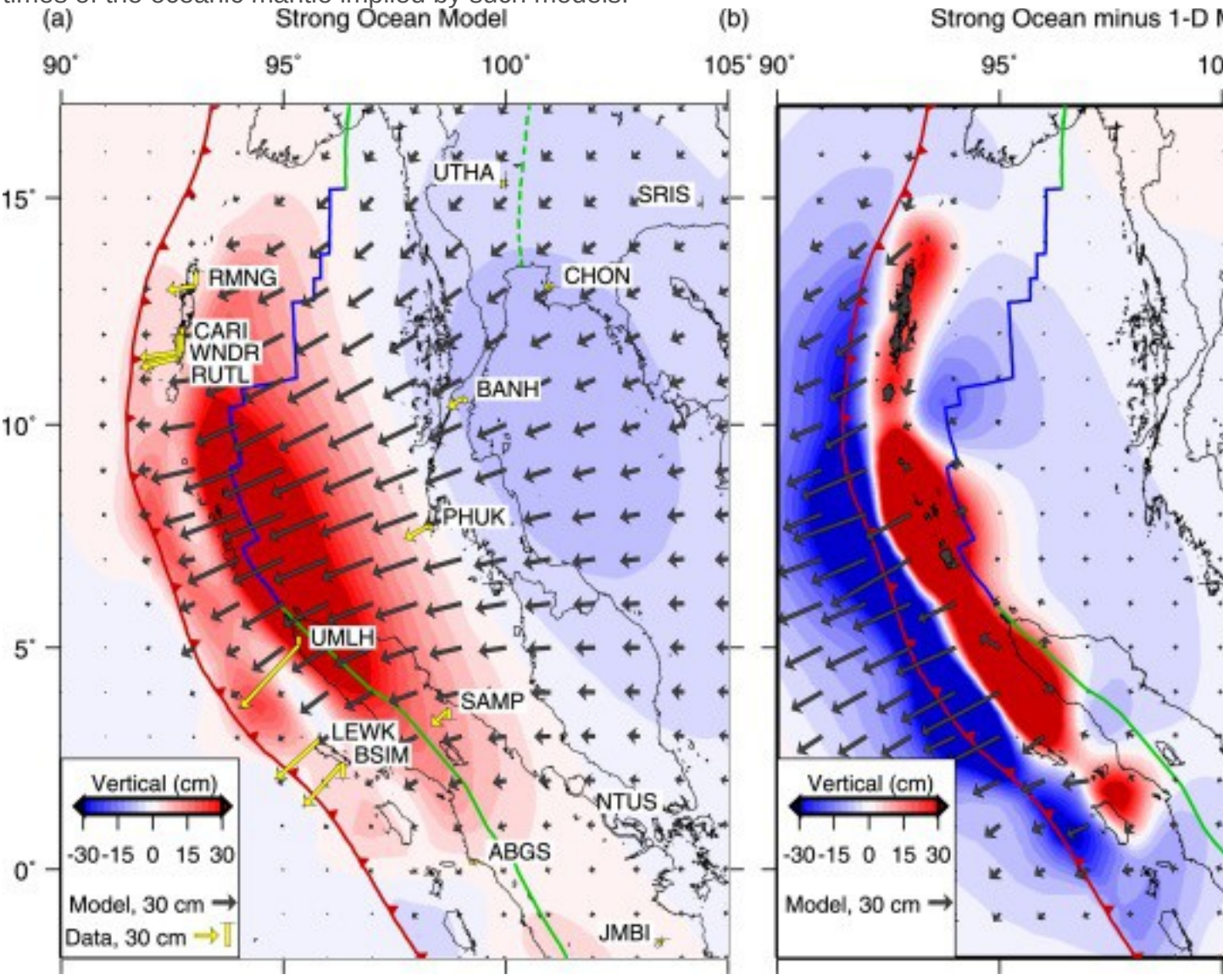

1. Download high-res image (966KB)
2. Download full-size image

Fig. 9. (a) Five years of cumulative viscoelastic relaxation from the 2004, 2005, and 2007 megathrust earthquakes using a model with ten times higher viscosity of the mantle underlying the ocean lithosphere seaward of the subducting slab. (b) The difference between the strong ocean earth model and the 1-D earth model cumulative viscoelastic relaxation.

4.4. Back-arc model

The low-viscosity back-arc region adds southwest oriented deformation under the Andaman Sea, uplift just east of the Andaman Islands, and a broad zone of subsidence between the Andaman transform and rift system and Thailand (Fig. 10c). There is only a slight difference observed at the Thai and Malaysian sites, but the GPS station locations are not optimally placed to observe a low-viscosity back-arc spreading center. The effects of the low-viscosity zone would be amplified if we shallow its upper depth limit or increase the viscosity contrast with the continental mantle. The Nicobar Islands would be the best location for observing this feature, and unpublished data from a campaign GPS station CBAY on Great Nicobar Island (230 km NW of Banda Aceh) experienced >25 cm of near-linear uplift between 2005 and 2012 (Joshi Catherine and Vineet Gahalaut, written comm., 2013), consistent with the substantial uplift predicted by models involving a low-viscosity backarc (Fig. 10). 2005 to 2013 uplift of other stations along the Andaman and Nicobar Islands during this period range from <5 cm to 40 cm (Paul et al., 2014). The steady subsidence observed at station SAMP in northern Sumatra (Fig. S3) that is not predicted by any of our models suggests that the weak backarc zone may extend further south than in our model.

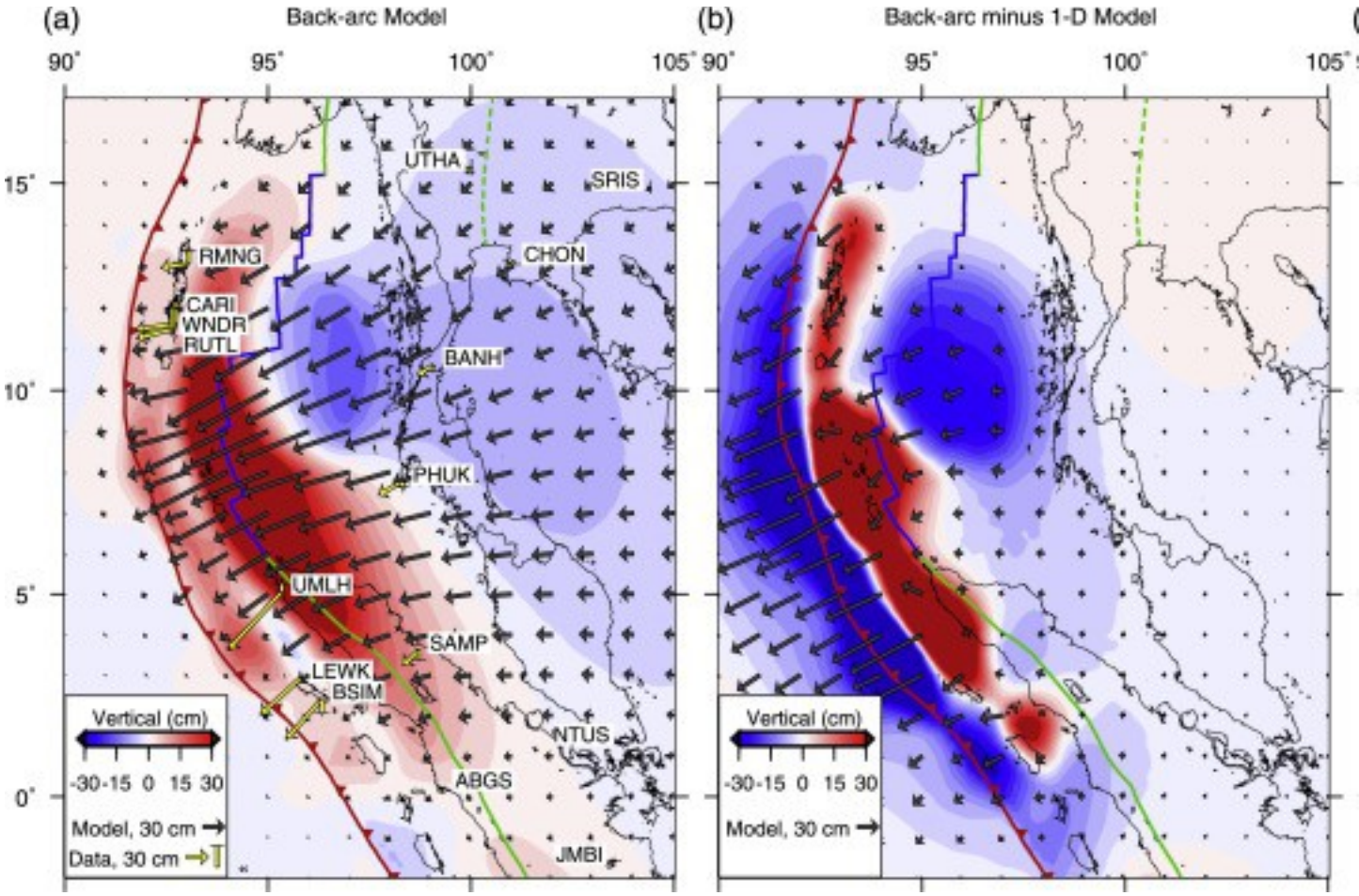

1. Download high-res image (1MB)
2. Download full-size image

Fig. 10. (a) Five years of cumulative viscoelastic relaxation from the 2004, 2005, and 2007 megathrust earthquakes using a model that adds a low-viscosity back-arc zone to the 3-D earth model (Fig. 6). (b) The difference between the back-arc earth model and the 1-D earth model cumulative viscoelastic relaxation. (c) The difference between the back-arc earth model and the strong ocean earth model (Fig. 9) cumulative viscoelastic relaxation.

5. Discussion

The early postseismic period after each of the megathrust earthquakes is characterized by a rapidly decaying transient, especially at the near-field sites (e.g., see time series for CARI in Fig. S7). We are not fitting this decaying early transient with our linear Maxwell rheology and focus on comparing model time series with observations starting about one year after the mainshock rupture. It may be appropriate to use a bi-viscous rheology that includes a transient viscosity, such as the Burgers body model used in several previous studies (Panet et al., 2010; Pollitz et al., 2008; Hoechner et al.,

2011, Hu and Wang, 2012) or consider models involving a power-law rheology appropriate for viscous flow by dislocation creep (Freed and Bürgmann, 2004). In addition, afterslip and poroelastic rebound are likely to have contributed locally to the early postseismic deformation, depending on the distribution of velocity strengthening behavior along the megathrust and permeability in the lithosphere.

Given the sparse sampling of the surface deformation field, we do not attempt to solve for an afterslip model to further improve the fit to the data. Aseismic afterslip has been observed in many tectonic environments following large earthquakes, although the magnitude and duration of the afterslip vary widely (e.g. Melbourne et al., 2002, Johanson et al., 2006). Based on the large stresses imparted to the transition zones updip and downdip of the coseismic ruptures, aseismic afterslip is expected to follow the Andaman–Sunda megathrust earthquakes and could also help to explain some of the early postseismic transients. Gahalaut et al. (2008) and Paul et al. (2012) have argued that significant afterslip is necessary to fit the Andaman Island postseismic observations. Paul et al. (2012) attempt to fit the 2008.5–2010.5 Andaman observations with a combination of viscoelastic relaxation and afterslip. Their preferred model includes ∼0.5 m/yr of afterslip located beneath and downdip of the Andaman Islands, and viscoelastic relaxation assuming a 90-km-thick elastic lithosphere and 3×10^{17} Pas asthenosphere. Their steady-state mantle viscosity is much lower than that found in other studies (e.g. Hu and Wang, 2012, Panet et al., 2010) and their model would not fit the observations in the far field. Hu and Wang (2012) find that introducing both a low transient viscosity in the mantle wedge and down-dip afterslip allows for a good fit to early and later GPS data. Starting in 2006, our strong ocean model fits the northern and southern Andaman Island and Car Nicobar observations very well, primarily within uncertainties. CARI, HAV2 and other stations in the middle Andaman Islands, have unaccounted for uplift and southward motion, suggesting there may still be some localized afterslip affecting these stations.

Hughes et al. (2010) rely on independent constraints on the 3-D permeability structure of the Andaman–Sunda subduction zone to show that postseismic deformation from poroelastic rebound is localized to within ∼200 km of the coseismic ruptures and is expected to be complete several months after the earthquakes. Poroelastic rebound predicts large subsidence near the trench and substantial surface uplift along the down-dip edge of the ruptures. Thus, this process is likely to have contributed some of the early postseismic uplift observed along the Andaman–Nicobar–Sumatra forearc islands, but does not produce significant displacements at greater distances.

6. Conclusions

It is important to consider three-dimensional variations in mantle rheology when modeling postseismic relaxation following great subduction zone earthquakes. We consider near-field and far-field GPS displacement time series spanning a five-year period starting with the 2004 Sumatra–Andaman earthquake to evaluate predicted postseismic displacement fields from a number of first-order rheologic earth models. Adding a rigid slab and viscosity contrast across the subducting oceanic plate produces a reversal in the predicted vertical motions along the forearc island chain reaching from the Andaman Islands to Sumatra, improves the fit to the near-field horizontal motions, and correctly predicts the lack of substantial postseismic displacements in southern India. This allows for one postseismic mechanism to correctly produce the orientation of the observations at sites located in the near-field, intermediate-field and far-field. More rapid motions immediately following the mainshocks suggest additional contributions from afterslip and poroelastic rebound and a lower effective mantle-wedge viscosity during an early transient relaxation period. Our models show that it is possible to fit the postseismic observations primarily with viscoelastic relaxation in a heterogeneous earth structure that is consistent with the thermal structure inferred from seismic tomographic data (Shapiro et al., 2008).

Acknowledgments

This work has been supported by NSF grants EAR-0738299 and EAR-1246850 (to R.B.). We acknowledge very helpful comments by two anonymous reviewers. The figures in this paper were produced using the GMT software. This is Berkeley Seismological Laboratory contribution 2015-09.

Appendix A. Supplementary material

The following is the Supplementary material related to this article.

Download Word document (7MB)Help with docx files

Figs. S1–S7. Time series of observed and modeled postseismic displacements from the 2004, 2005 and 2007 megathrust earthquakes along the Andaman–Sunda subduction zone. We consider available horizontal and vertical campaign and continuous GPS observations from the Andaman, Nicobar, and Sumatran forearc islands, mainland Sumatra, Thailand, the Malay Peninsula, the Indian Ocean, and southern India, spanning five years of postseismic deformation. Interseismic velocities and coseismic offsets have been removed from the data. See main text for description of the four models that are compared with the data.

References

Apel, 2011

E.V. Apel**Shells on a sphere: tectonic plate motion and plate boundary deformation**

PhD thesis

University of California, Berkeley (2011)

Avouac, 2015

J.P. Avouac**From geodetic imaging of seismic and aseismic fault slip to dynamic modeling of the seismic cycle**

Annu. Rev. Earth Planet. Sci., 43 (2015), 10.1146/annurev-earth-060614-105302

Banerjee et al., 2007

P. Banerjee, F.F. Pollitz, B. Nagarajan, R. Bürgmann**Coseismic slip distributions of the 26 December 2004 Sumatra–Andaman and 28 March 2005 Nias earthquakes from GPS static offsets**

Bull. Seismol. Soc. Am., 97 (2007), pp. S86-S102

CrossRefView Record in Scopus

Broerse et al., 2015

T. Broerse, R. Riva, W. Simons, R. Govers, B. Vermeersen**Postseismic GRACE and GPS observations indicate a rheology contrast above and below the Sumatra slab**

J. Geophys. Res., 120 (2015), pp. 5343-5361

CrossRefView Record in Scopus

Bürgmann and Dresen, 2008

R. Bürgmann, G. Dresen**Rheology of the lower crust and upper mantle: evidence from rock mechanics, geodesy and field observations**

Annu. Rev. Earth Planet. Sci., 36 (2008), pp. 531-567, 10.1146/annurev.earth.36.031207.124326

CrossRefView Record in Scopus

Chlieh et al., 2007

M. Chlieh, J. Avouac, V. Hjorleifsdottir, T.A. Song, C. Ji, K. Sieh, A. Sladen, H. Hebert, L.Prawirodirdjo, Y. Bock, J. Galetzka**Coseismic slip and afterslip of the great Mw 9.15 Sumatra–Andaman earthquake of 2004**

Bull. Seismol. Soc. Am., 97 (2007), pp. S152-S173

CrossRefView Record in Scopus

Curray, 2005

J. Curray**Tectonics and history of the Andaman Sea region**

J. Asian Earth Sci., 25 (2005), pp. 187-232

ArticleDownload PDFView Record in Scopus

Freed and Bürgmann, 2004

A.M. Freed, R. Bürgmann**Evidence of powerlaw flow in the Mojave desert mantle**

Nature, 430 (2004), pp. 548-551, 10.1038/nature02784

CrossRefView Record in Scopus

Gahalaut et al., 2008

V.K. Gahalaut, S. Jade, J.K. Catherine, R. Gireesh, M.B. Ananda, P.D. Kumar, M.Narsaiah, S.S.H. Jafri, A. Ambikapathy, A. Bansal, R.K. Chadha, D.C. Gupta, B. Nagarajan, S. Kumar**GPS measurements of postseismic deformation in the Andaman–Nicobar region following the giant 2004 Sumatra–Andaman earthquake**
J. Geophys. Res., 113 (2008), Article B08401

Hashimoto et al., 2006

M. Hashimoto, N. Choosakul, M. Hashizume, S. Takemoto, H. Takigucki, Y. Fukuda, K.Fujimori**Crustal deformations associated with the great Sumatra–Andaman earthquake deduced from continuous GPS observation**
Earth Planet. Space, 58 (2006), pp. 127-139
CrossRefView Record in Scopus

Hayes et al., 2012

G.P. Hayes, D.J. Wald, R.L. Johnson**Slab1.0: a three-dimensional model of global subduction zone geometries**
J. Geophys. Res., 117 (2012), Article B01302

Hoechner et al., 2011

A. Hoechner, S.V. Sobolev, I. Einarsson, R. Wang**Investigation on afterslip and steady state and transient rheology based on postseismic deformation and geoid change caused by the Sumatra 2004 earthquake**
Geochem. Geophys. Geosyst., 12 (7) (2011), Article Q07010, 10.1029/2010GC003450

Hsu et al., 2006

Y. Hsu, M. Simons, J. Avouac, J. Galetzka, K. Sieh, M. Chlieh, D. Natawidjaja, L. Prawirodirdjo, Y. Bock**Frictional afterslip following the 2005 Nias–Simeulue earthquake, Sumatra**
Science, 312 (2006), pp. 1921-1926
CrossRefView Record in Scopus

Hu - and - Wang

,
2012

Y. Hu, K. Wang**Spherical-Earth finite element model of short-term postseismic deformation following the 2004 Sumatra earthquake**
J. Geophys. Res., 117 (2012), 10.1029/2012JB009153

Hu et al., 2004

Y. Hu, K. Wang, J. He, J. Klotz, G. Khazaradze**Three-dimensional viscoelastic finite element model for postseismic deformation of the great 1960 Chile earthquake**
J. Geophys. Res., 109 (2004)
http://dox.doi.org/10.1029/2004JB003163

Hughes et al., 2010

K.L.H. Hughes, T. Masterlark, W.D. Mooney**Poroelastic stress-triggering of the 2005 M8.7 Nias earthquake by the 2004 M9.2 Sumatra–Andaman earthquake**
Earth Planet. Sci. Lett., 293 (2010), pp. 289-299
ArticleDownload PDFView Record in Scopus

Johanson et al.,

I.A. Johanson, E.J. Fielding, F. Rolandone, R. Burgmann**Coseismic and postseismic slip of the 2004 Parkfield earthquake from space-geodetic data**
Bull. Seismol. Soc. Am., 96 (2006), pp. S1-S13

Konca et al., 200

A.O. Konca, V. Hjorleifsdottir, T.A. Song, J. Avouac, D.V. Helmberger, C. Ji, K. Sieh, R.Briggs, A. Meltzner**Rupture kinematics of the 2005 Mw 8.6 Nias–Simeulue earthquake from the joint inversion of seismic and geodetic data**
Bull. Seismol. Soc. Am., 97 (2007), pp. S307-S322
CrossRefView Record in Scopus

Konca et al., 200

A.O. Konca, J. Avouac, A. Sladen, A.J. Meltzner, K. Sieh, P. Fang, Z. Li, J. Galetzka, J.Genrich, M. Chlieh, D.H. Natawidjaja, Y. Bock, E.J. Fielding, C. Ji, D.V. Helmberger**Partial rupture of a locked patch of the Sumatra megathrust during the 2007 earthquake sequence**
Nature, 465 (2008), pp. 631-635
CrossRefView Record in Scopus

Melbourne et al.,

T.I. Melbourne, F.H. Webb, J.M. Stocl, C. Reigber**Rapid postseismic transients in subduction zones from continuous GPS**
J. Geophys. Res., 107 (2002), p. 2241

Müller et al., 199

R.D. Müller, W.R. Roest, J.-Y. Royer, L.M. Gahagan, J.G. Sclater**Digital isochrons of the world's ocean floor**
J. Geophys. Res., 102 (1997), pp. 3211-3214
CrossRefView Record in Scopus

Ogawa and Heki

R. Ogawa, K. Heki**Slow postseismic recovery of geoid depression formed by the 2004 Sumatra–Andaman earthquake by mantle water diffusion**
Geophys. Res. Lett., 34 (2007), Article L06313, 10.1029/2007GL029340
View Record in Scopus

Panet et al., 201

I. Panet, F. Pollitz, V. Mikhailov, M. Diament, P. Banerjee, K. Grijalva**Upper mantle rheology from GRACE and GPS postseismic deformation after the 2004 Sumatra–Andaman earthquake**
Geochem. Geophys. Geosyst., 11 (2010), Article Q06008

Panumastrakul e

E. Panumastrakul, W.J.F. Simons, C. Satirapod**Modeling post-seismic displacements in Thai geodetic network due to the Sumatra–Andaman and Nias earthquakes using GPS observations**
Surv. Rev., 44 (2012), pp. 72-77
CrossRefView Record in Scopus

Paul et al., 2007

J. Paul, A.R. Lowry, R. Bilham, S. Sen, R. Smalley Jr.**Postseismic deformation of the Andaman Islands following the 26 December, 2004 Great Sumatra–Andaman earthquake**
Geophys. Res. Lett., 34 (2007), Article L19309, 10.1029/2007GL031024

Paul et al., 2012

J. Paul, C.P. Rajendran, A.R. Lowry, V. Andrade, K. Rajendran**Andaman postseismic deformation observations: still slipping after all these years?**
Bull. Seismol. Soc. Am., 102 (2012), pp. 343-351
CrossRefView Record in Scopus

Paul et al., 2014

J. Paul, K. Rajendran, C.P. Rajendran**Slow slip acceleration beneath Andaman Islands triggered by the 11 April 2012 Indian Ocean earthquakes**
Bull. Seismol. Soc. Am., 104 (2014), pp. 1556-1561
CrossRefView Record in Scopus

Paulson et al., 2

A. Paulson, S. Zhong, J. Wahr**Modelling post-glacial rebound with lateral viscosity variations**
Geophys. J. Int., 163 (2005), pp. 357-371
CrossRefView Record in Scopus

Pollitz et al., 200

F. Pollitz, R. Bürgmann, P. Banerjee**Postseismic relaxation following the great 2004 Sumatra–Andaman earthquake on a compressible self-gravitating Earth**
Geophys. J. Int., 167 (2006), 10.1111/j.1365-1246X.2006.03018.x

Pollitz et al., 200

F.F. Pollitz, P. Banerjee, K. Grijalva, B. Nagarajan, R. Bürgmann**Effect of 3-D viscoelastic structure on post-seismic relaxation from the 2004 M = 9.2 Sumatra earthquake**
Geophys. J. Int., 173 (2008), pp. 189-204
CrossRefView Record in Scopus

Shapiro and Ritz

N.M. Shapiro, M.H. Ritzwoller**Thermodynamic constraints on seismic inversions**
Geophys. J. Int., 157 (2004), pp. 1175-1188, 10.1111/j.1365-246X.2004.02254.x
CrossRefView Record in Scopus

Shapiro et al., 20

N. Shapiro, M. Ritzwoller, E. Engdahl**Structural context of the great Sumatra–Andaman Islands earthquake**
Geophys. Res. Lett., 35 (2008), Article L05301

Shearer and Bür

P.M. Shearer, R. Bürgmann**Lessons learned from the 2004 Sumatra–Andaman megathrust rupture**
Annu. Rev. Earth Planet. Sci., 38 (2010), pp. 103-131
CrossRefView Record in Scopus

Subarya et al., 2

C. Subarya, M. Chlieh, L. Prawirodirdjo, J. Avouac, Y. Bock, K. Sieh, A.J. Meltzner, D.H.Natawidja ja, R. McCaffrey**Plate-boundary deformation associated with the great Sumatra–Andaman earthquake**
Nature, 440 (2006), pp. 46-51
CrossRefView Record in Scopus

Vigny et al., 2005

C. Vigny, W.J.F. Simons, S. Abu, R. Bamphenyu, C. Satirapod, N. Choosakul, C. Subarya, A.Soc quet, K. Omar, H.Z. Abidin, B.A.C. Ambrosius**Insight into the 2004 Sumatra–Andaman earthquake from GPS measurements in southeast Asia**
Nature, 436 (2005), pp. 201-206
CrossRefView Record in Scopus

Wang, 2007

K. Wang**Elastic and viscoelastic models of crustal deformation in subduction earthquake cycles**
T.H. Dixon, J.C. Moore (Eds.), The Seismogenic Zone of Subduction Thrust Faults, Columbia University Press (2007)

Wang et al., 201

K. Wang, Y. Hu, J. He**Deformation cycles of subduction earthquakes in a viscoelastic Earth**
Nature, 484 (7394) (2012), pp. 327-332
CrossRefView Record in Scopus